Preliminary Analysis of Seismicity Near Eagleton 1-29, Carter County, July 2014

Amberlee Darold, Austin A. Holland, Chen Chen, Amie Youngblood

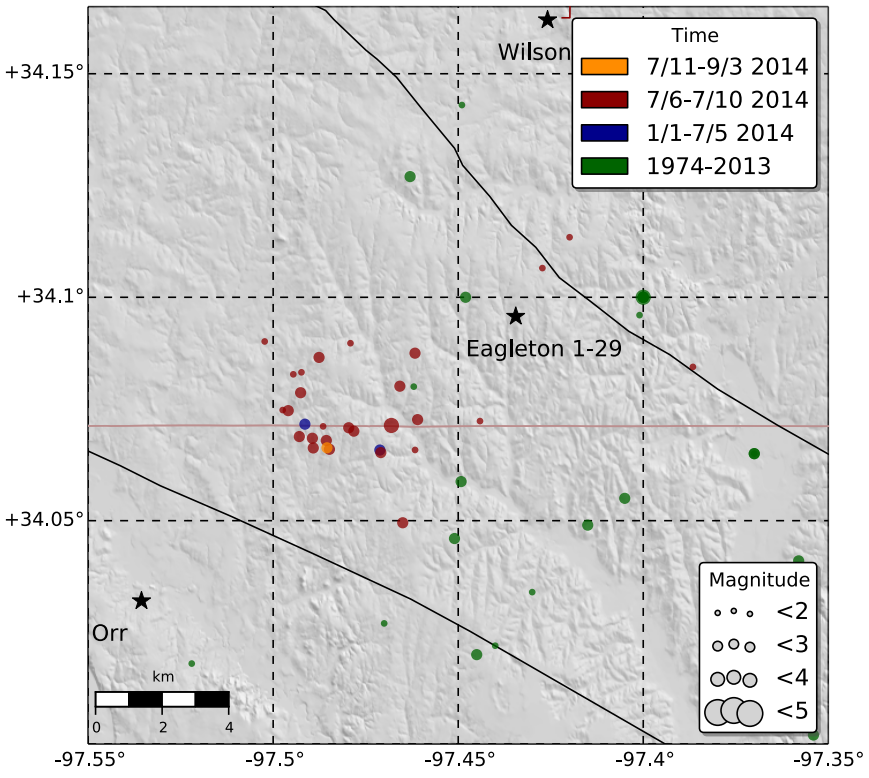

Oklahoma Geological Survey
Open-File Report
OF2-2014
September 4, 2014

OKLAHOMA GEOLOGICAL SURVEY
Open-file Report Disclaimer

This Open-file Report is intended to make the results of research available at the earliest possible date and is intended as a preliminary report not as a final publication.

Suggested Citation:

Darold, A., A. A. Holland, C. Chen, and A. Youngblood (2014), Preliminary Analysis of Seismicity Near Eagleton 1-29, Carter County, July 2014, *Okla. Geol. Surv. Open-File Report*, *OF2-2014*, 17.

Oklahoma Geological Survey
Sarkeys Energy Center
100 East Boyd St., Rm. N-131
Norman, Oklahoma 73019-0628

Summary

On July 8th 2014, we, The Oklahoma Geologic Survey were notified by the Oklahoma Corporation Commission (OCC) that they had received an email indicating possible seismic activity associated with the hydraulic fracturing of the Eagleton 1-29 well located in Section 29 5S 2W in southern Carter County, Oklahoma.

While this area of Oklahoma has a low level of background seismicity, about 10 located events per year, there have been 43 earthquakes located in the area for 2014. We were aware of an increase in earthquakes occurring in this area however, we were not aware of the hydraulic fracturing of Eagleton 1-29. Of the recent events, 26 coincide, in time and space, with the 2-day hydraulic fracturing of Eagleton 1-29 occurring July 7th through July 8th, 2014. The largest event located during this sequence, at approximately 9:38 am on July 7th, 2014, was a magnitude 3.2ML located ~ 4.5 km southwest of the well at ~7.3 km depth. The majority of events that have been located in this sequence are measured under magnitude 2.5ML, occur at depths of ~ 3.5 to 8.5 km (~ 11,483 to 27,887 ft.) and are within 1-7 km from the well. The OCC provided us with pumping curves for the four-stage stimulation of the vertical well with a total depth of ~ 3.54 km (11,616 ft.) beginning the morning of July 7th, 2014 and ending the evening of July 8th, 2014. By plotting the pressures measured at wellhead and the discharge rate (injection rate) through time we are able to see a strong correlation with the local seismicity and stimulation of Eagleton 1-29.

We find a strong temporal correlation between injection in the Eagleton 1-29 and the occurrence of earthquakes that is clearly distinct from the background rate of seismicity. This and the relatively close spatial proximity do suggest a causal link between hydraulic fracturing and the 26 earthquakes located near the well during the four stages of hydraulic fracturing. What remains to be explained is the distance between the stimulated well and the earthquakes. Greater geotechnical information will be required to both address our earthquake location uncertainties as well as geomechanical considerations as to how this sequence of earthquakes may have been triggered by hydraulic fracturing and what information we can ascertain about Earth properties in the area from this occurrence. This area has been and may continue to be seismically active, this analysis should be considered preliminary and with ongoing seismicity and research our understanding of this seismicity could change. The plot below shows the temporal correlations, in UTC, of the 26 earthquakes coincident with the four stages of hydraulic fracturing of the Eagleton 1-29 well.

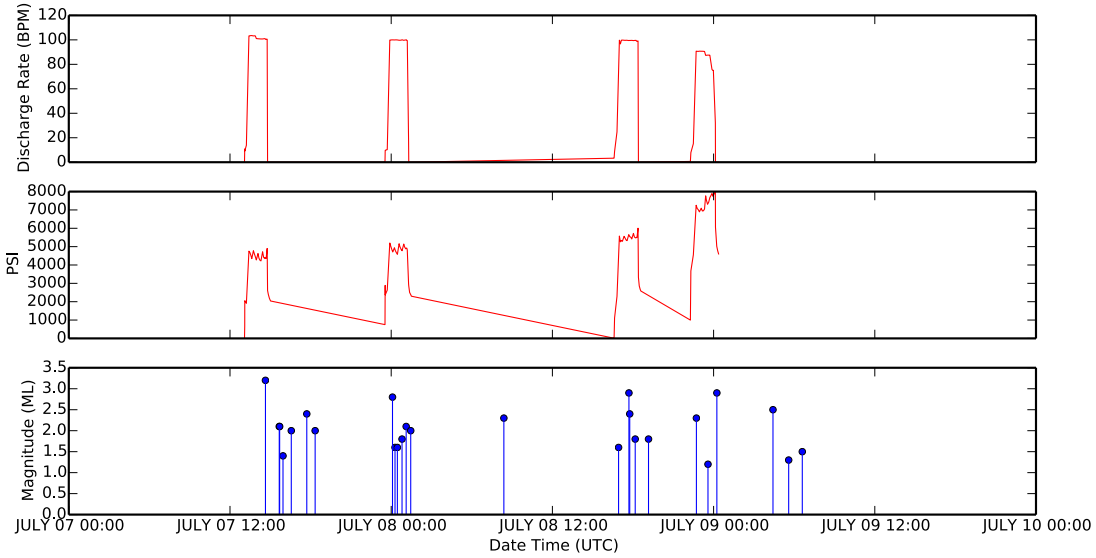

Introduction

On July 8th, we, The Oklahoma Geologic Survey (OGS) were notified by the Oklahoma Corporation Commission (OCC) that they had received an email indicating possible seismic activity associated with the hydraulic fracturing of the Eagleton 1-29 well located in Section 29 5S 2W in southern Carter County, Oklahoma.

While this area of Oklahoma has a low level of background of seismicity, about 10 located events per year, there have been 43 earthquakes located in the area for 2014 (Figure 1). We were aware of an increase in earthquakes occurring in this area however, we were not aware of the hydraulic fracturing of Eagleton 1-29. Of the recent events, 26 coincide, in time and space, with the hydraulic fracturing of Eagleton 1-29, July 7th through July 9th, 2014, UTC. The OCC provided us with the pumping curves for the stimulation of the Eagleton 1-29.

In this study, we will address the seismicity coincident with the hydraulic fracturing of Eagleton 1-29 as the Wilson 2014 sequence, centered 6 miles southwest of Wilson, Oklahoma. The study area includes the area between latitudes 33.95N and 34.20N and longitudes 97.6W and 97.25W. Also, included in this report is the derivation of the local magnitude scale used by the OGS in Appendix A.

This report will document the background seismicity and the recent swarm, Wilson 2014, coinciding with the hydraulic fracturing of Eagleton 1-29 well. This area has been and may continue to be seismically active this analysis should be considered preliminary and with ongoing seismicity and research our understanding of this seismicity could change.

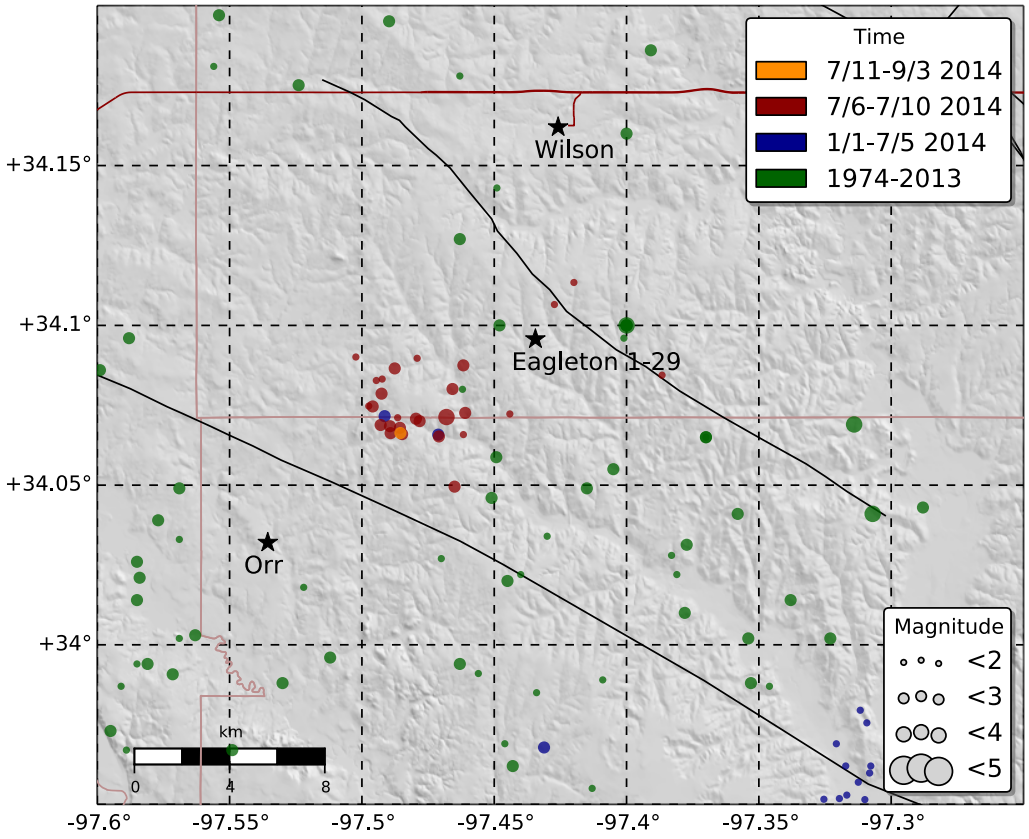

Figure 1. Cumulative map of located earthquakes occurring in southwestern Carter County and northwestern Love County from 1974 to 09/04/2014. Mapped faults shown with solid black lines (Cardott, personal communication, 2014) county lines in pink and U.S. highways in red.

Regional Seismic Network

The OGS operates a regional seismic network of 15 permanent stations and 17 temporary stations throughout Oklahoma. We also bring in data from Kansas, Arkansas, and Texas operated by the United States Geologic Survey (USGS), Central and Eastern US Network EarthScope USArray and State Surveys (Figure 2). We receive data in real-time to the OGS earthquake data processing system for all stations shown in Figure 2. There are currently four temporary, continuously recording seismic stations operating within central Love County, deployed in response to the Love County earthquake sequence of September 2013 (Holland, 2013a), located to the southeast of the Wilson 2014 Sequence. There are two continuously recording OGS permanent stations to the northwest of the sequence and one Central and Eastern US Network EarthScope USArray station to the south in Texas that have aided in obtaining reliable locations for these events (Figure 3).

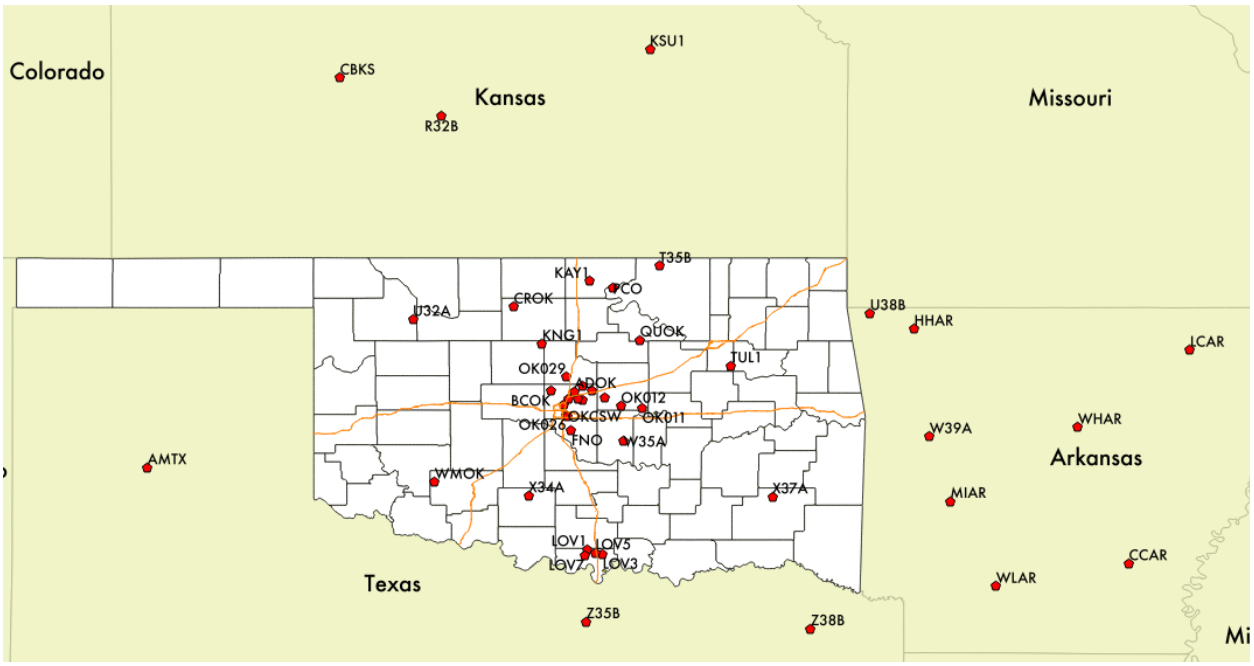

Figure 2. Seismic stations from the OGS regional network, USGS network, Central and Eastern US Network EarthScope USArray and State Survey stations, through Arkansas, Kansas, Oklahoma and Texas, utilized in locating earthquakes in Oklahoma, denoted with red pentagons.

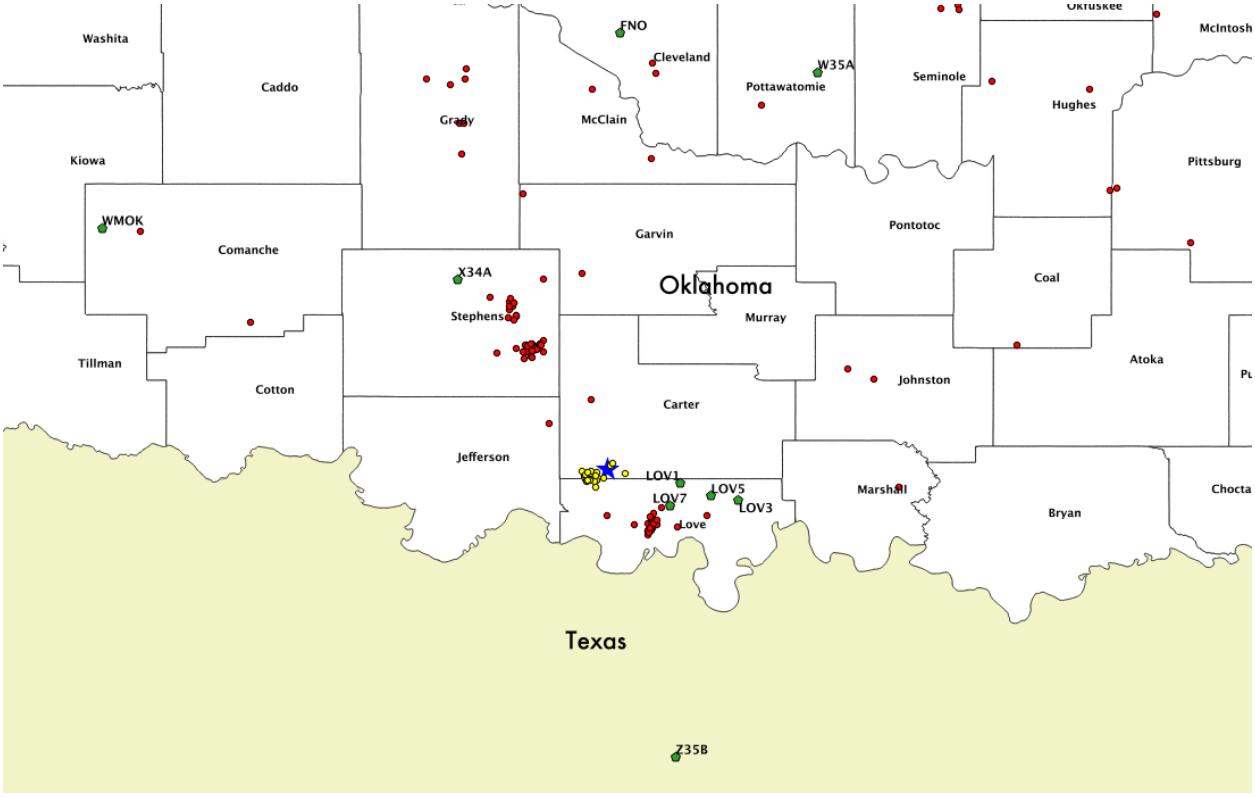

Figure 3. Stations closest to the Wilson 2014 sequence plotted with green pentagons. WMOK, W34A, FNO, and W35A are permanent OGS station, LOV1, LOV3, LOV5, and LOV7 are temporary OGS stations and Z35B is a Central and Eastern US Network EarthScope USArray station. Yellow dots are earthquakes coincident with the hydraulic fracturing of the Eagleton 1-29 well, denoted with a blue star. Red dots are earthquakes located from 01/01/2014 through 09/04/2014.

Eagleton 1-29

The Eagleton 1-29 is a vertical well completed to a total depth of ~3.5 km (11,574 ft.). The well was stimulated by four stages of hydraulic fracturing beginning on July 7th, 2014 and ending July 9th, 2014. The well is located in the SE quarter of the NW quarter of Section 29 Township 5S Range 2W at 34.095728° N latitude and 97.434442° W longitude.

Stage 1 began at 13:04:48 UTC on July 7th and ended at 15:01:09 UTC on July 7th.
Depths: ~ 3.53 km – 3.44 km (11547 ft. – 11295 ft.)
Stage 2 began at 23:32:18 UTC on July 7th and ended at 01:30:15 UTC on July 8th.
Depths: ~ 3.43 km – 3.35 km (11230 ft. – 11005 ft.)
Stage 3 began at 16:35:32 UTC on July 8th and ended at 18:34:56 UTC on July 8th.
Depths: ~ 3.34 km – 3.23 km (10971 ft. – 10826 ft.)
Stage 4 began at 22:16:20 UTC on July 8th and ended at 00:22:24 UTC on July 9th.
Depths: ~ 3.29 km – 3.22 km (10797 ft. – 10558 ft.)

Wilson 2014 Sequence

This area has background seismicity with known clusters of earthquakes. The number of earthquakes large enough to be located by the OGS regional network range from 0-10 (average) yearly events spanning both Carter and Love counties between the years of 1974 to 2012. In 2013 there was a spike of 81 events, largely associated with the Love County Swarm of September 2013, addressed in the OGS Open File Repot: OF1-2013V2013.9.30. Already in 2014 there have been 58 events within the two counties; 43 of these events are located in our study area and 26 are coincident with the stimulation of Eagleton 1-29 and are within a distance of 7.0 km to the well (Figure 1). The Wilson 2014 Sequence lies between two mapped parallel northwest trending faults associated with the Wichita Uplift (Figure 1., Cardott, personal communication, 2014); it is unclear at this point if these events are occurring on these faults or on associated structures.

By plotting the pressures measured at wellhead and the discharge rate (injection rate) through time we are able to see a strong correlation with seismicity (Figure 4). The largest event located during the Wilson 2014 sequence was a magnitude 3.2ML, located ~ 4.5 km southwest of the well at ~7.3 km depth, this event occurred at 14:38 July 7th, 2014 UTC, soon after stimulation began. Most of the events that have been located in this sequence are under magnitude 2.5ML. We can see from Figure 5, that the events occur in a range of 1-7 km from the well and do not have a clear trend or move out from the well location with time. There is also no clear trend with the inter-event distances however, the inter-event times shows that earthquakes concurrent with the stages of hydraulic fracturing happened rapidly with very little time spanned between events.

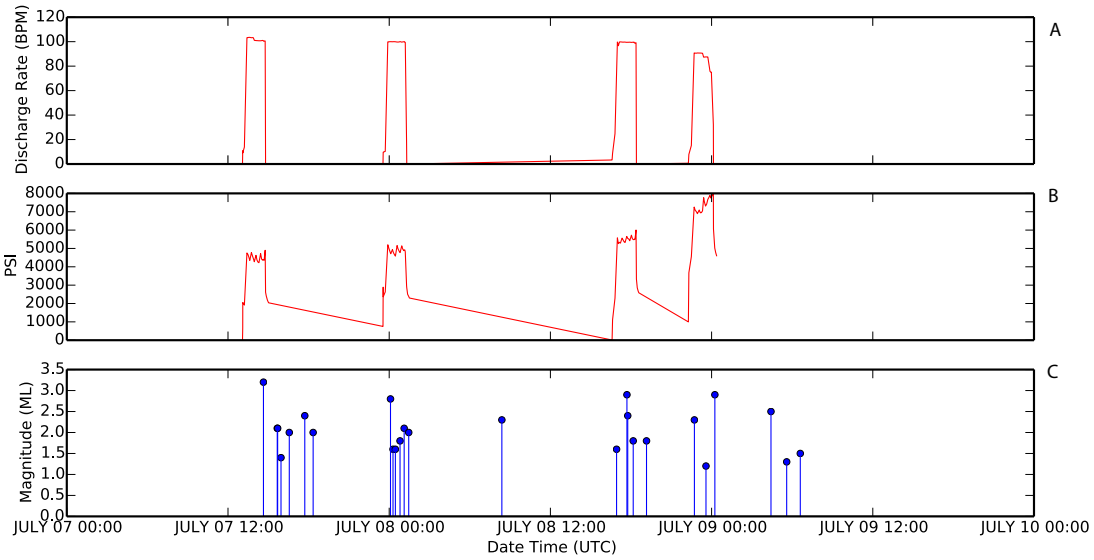

Figure 4. The plots span, in UTC time, the four hydraulic fracturing stages of Eagleton 1-29 well between July 7th 2014 and July 9th 2014. Plot A shows the discharge rate in BPM, or rate of injection, through time, plot B shows the pressure in PSI through time and plot C shows magnitude of earthquakes occurring within 7.0 km of the Eagleton well through time.

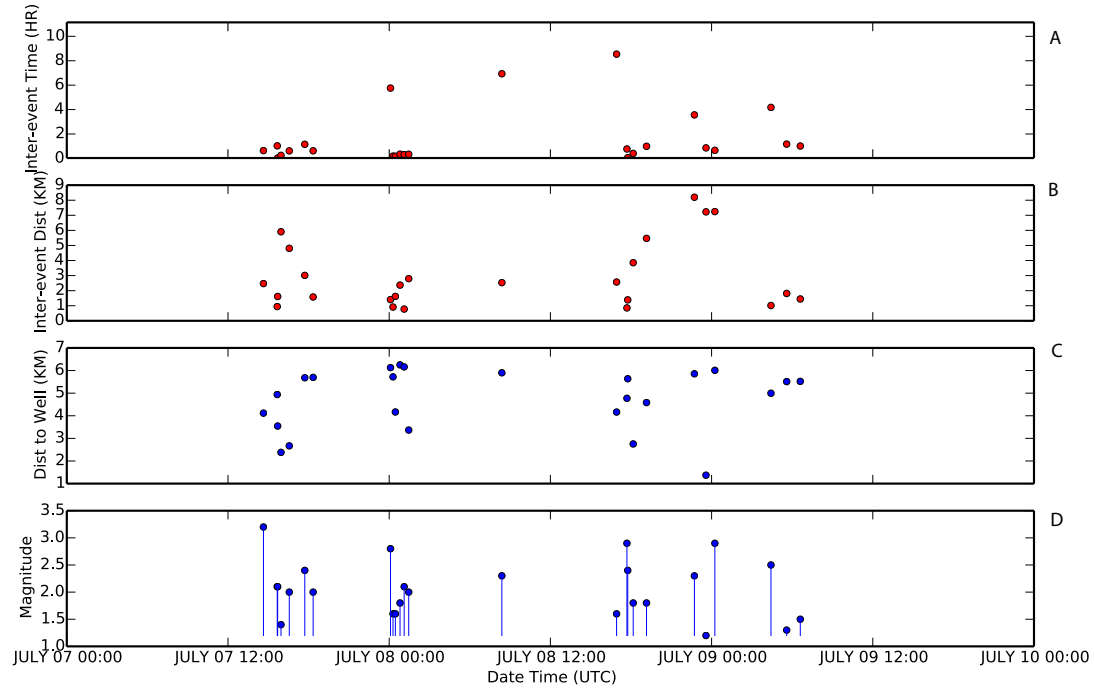

Figure 5. The plots span, in UTC time, the four hydraulic fracturing stages of Eagleton 1-29 well between July 7th 2014 and July 9th 2014. Plot A shows the inter-event timing in hours between successive events, plot B shows the inter-event distance in km between

successive events, plot C shows event distance from well in km, and plot D shows magnitude of events through time.

Methods

Routine earthquake locations are computed using the SEISAN Analysis software (Havskov and Ottemoller, 1999). Providing single event locations with an average horizontal uncertainty of ~3 km and an average vertical uncertainty of ~3 km. From the single event locations we obtain an average depth of 5 km. We also routinely use SEISAN for the determination of magnitude. The primary magnitude reported by the OGS is local magnitude ML. The local calibration for the ML relationship was determined through the method described in Appendix A.

In addition we relocated all the earthquakes within the study region using HYPODD (Waldhauser and Ellsworth, 2000). HYPODD is joint relocation that takes advantage of small differences in phase travel paths between events, which are closely spaced and provide accurate relative locations. HYPODD improved locations and provided event locations with an average horizontal uncertainty of 0.7 km, an average vertical uncertainty of 1.3 km and an average depth of 5.0 km. Figure 6, shows the location differences with the HYPODD relocated events in the Wilson 2014 sequence. It is important to note that the uncertainty for single event locations from SEISAN and HYPODD are highly dependent both on distance to the nearest stations as well as number of phase observations. Also, note that figures 1, 3, 4, and 5 were plotted using event locations calculated from SEISAN.

Hypocenter locations for both methods are highly dependent on a number of factors. First, is the velocity model assumed for the earthquake locations. We use the regional Oklahoma velocity model, which is most likely not the most appropriate model for this area. The greatest effect to the location given the station coverage from the velocity model will be in the vertical direction. As such until a more detailed local velocity model can be established from sonic logs and potentially check-shot data, the greatest uncertainty is in the estimation hypocentral depth. This uncertainty is certainly larger than the formal uncertainties listed above. There is reasonably good regional seismic station coverage with the nearest station about 25 km from the center of the earthquake sequence and 6 stations within 90 km with fair azimuthal coverage (Figure 3.). For better control on earthquake focal depths seismic stations closer to the earthquake sequence would have been necessary. A 3D velocity model if close to accurate would also enhance vertical resolution of focal depths, but this effort could represent a very large effort with marginal gain depending on the quality of data used to constrain the model.

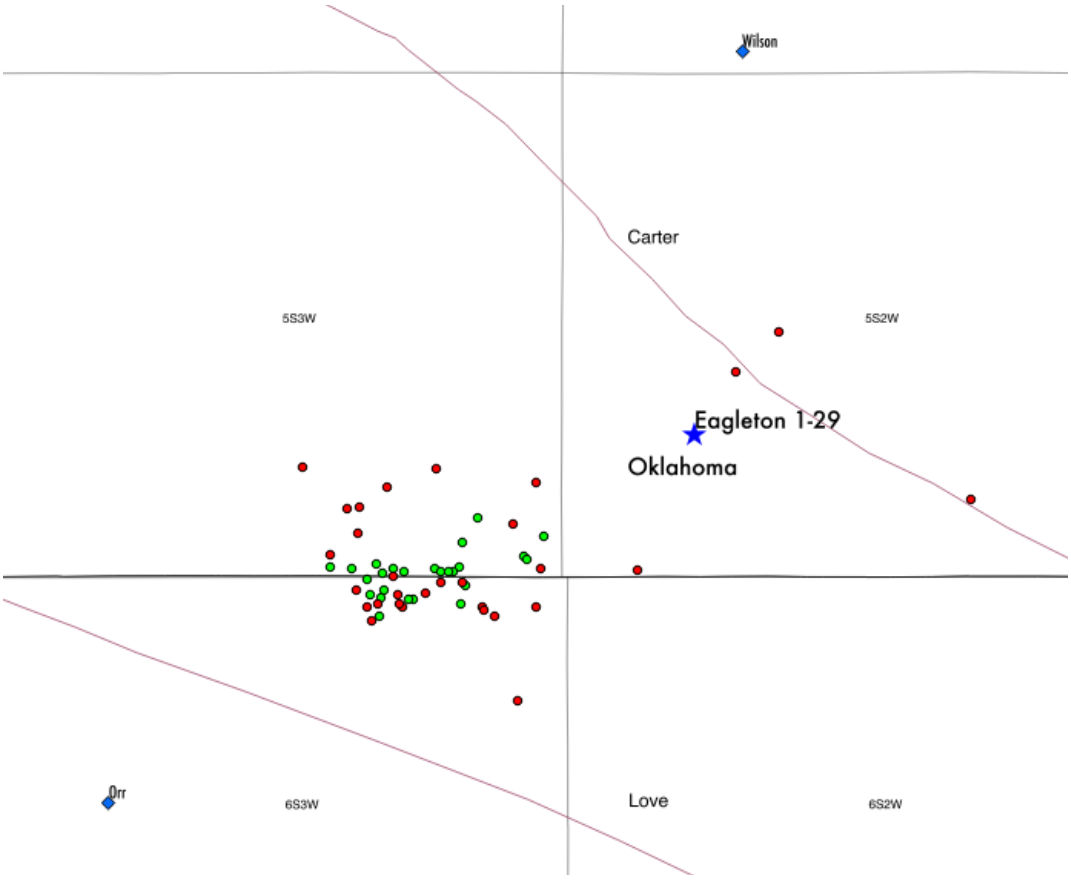

Figure 6. Comparison of SEISAN to HYPODD relocated events. SEISAN located event are shown in red and HYPODD relocated events are shown in green. Blue star denotes the Eagleton 1-29 well. Light red lines show mapped faults (Cardott, personal communication, 2014).

Earthquake Triggering from Fluid Injection

There have been a number of specific cases where the potential of induced seismicity has been suggested in and near Oklahoma over the past few years involving both hydraulic fracturing and disposal well activities (Brown et al., 2013; Frohlich, 2012; Frohlich et al., 2011; Holland, 2013; Holland et al., 2013; Horton, 2012; Keranen et al., 2013; Rubenstein et al., 2013). These examples include some damaging earthquakes up to a magnitude of 5.7 that have potentially been induced by fluid injection. In addition at least three earthquake swarms were identified on the Love/Carter county line in the late 1970's. From May 1, 1977, to December 31, 1978, 400 earthquakes were detected in Carter and Love County, most of these events were too small to locate. Following, there were two swarms potentially linked to commercial stimulation of deep wells near Wilson; June 23, 1978, there were 70 earthquakes in 6.2 hours and in May 1979 there were 90 earthquakes apparently coincident with the first two hydraulic fracturing stages of a well. Most of the events that were located, during this time, occurred in areas of active oil and gas production and could potentially have been caused by hydraulic fracturing, but no

definitive conclusion could be reached with the available data (Nicholson and Wesson, 1990).

Seismicity from oil and gas activities can be induced from either injection of fluids or removal of fluids, and both types of induced seismicity can be difficult to distinguish from naturally occurring seismicity (Suckale, 2009). Changes of stress within a producing field are much more difficult to know and modeling the response of a field to fluid extraction requires a great number of assumptions. Fluid injection should be the easiest to identify because the cause involves a known source location. In addition the diffusion of pore pressure within the Earth has long been recognized to be the triggering mechanism for fluid injection induced earthquakes (Fletcher and Sykes, 1977; Miller et al., 2004; Nicholson and Wesson, 1990; Nur and Booker, 1972; Ohtake, 1974; Rozhko, 2010; Shapiro et al., 1999; Talwani and Acree, 1985). The pore pressure diffusion model allows for the comparison of timing and spatial characteristics of fluid injection and earthquakes to provide an assessment of the likelihood of a given set of earthquakes to be induced by fluid injection. This has often worked well when evaluating the potential of a single well but can prove more difficult when multiple wells may be involved. However, the hydraulic diffusivity for most cases of triggered seismicity range from 0.1 to 10.0m^2/s (Talwani et al., 2007) while the first event of the Wilson 2014 sequence occurred within 100 minutes of initiation of injection and ~4.5km away from the well. The significant distance between stimulated well and earthquakes may not be out of the realm of a reasonable distance, but certainly represents an interesting observation that must be explained. Generally triggered seismicity is thought to occur on critically or near critically stressed faults, and most faults appear to be near critical stress (Zoback et al., 2002). Earthquakes triggered by hydraulic fracturing have only been suggested for a relatively small number of cases (Holland, 2013b).

Conclusions

There is a strong temporal correlation between injection associated with hydraulic fracturing of the Eagleton 1-29 and the occurrence of earthquakes that is clearly distinct from the background rates of seismicity. This and the relatively close spatial proximity do suggest a causal link between hydraulic fracturing and the Wilson 2014 earthquakes. What remains to be examined are the mechanisms by which this may have occurred. The distances at which the earthquakes occurred from the well are quite large for a delay of 100 minutes between the onset of hydraulic fracturing and the first earthquake. More geotechnical information will be required to both address velocity model uncertainties as well as geomechanical considerations as to how this sequence of earthquakes may have been triggered by hydraulic fracturing and what information we can ascertain about Earth properties in the area from this occurrence. Such information may help prevent such occurrences in the future.

Further Work

There are additional endeavors we can and are taking to improve this analysis. It is recognized that more small events occurred within this sequence and waveform cross-

correlation can be used to identify smaller earthquakes associated with this sequence to get a better understanding of the timing of seismicity. It will also be important to develop an advanced velocity model of this region to improve the locations and depths of all events located for this sequence. Furthermore, we need to evaluate the pore-pressure diffusion from the Eagleton 1-29 well by determining the hydraulic permeability and diffusivity of the geologic formations that the well intersects along with a greater understanding of the local fault structures.

References

Bakun, W. H., and Joyner, W. B., 1984, The ML Scale in Central California: Bull. Seismol. Soc. Am., v. 74, no. 5, p. 1827-1843.

Benz, H. M., Frankel, A., and Boore, D. M., 1997, Regional Lg Attenuation for the Continental United States: Bulletin of the Seismological Society of America, v. 87, no. 3, p. 606-619.

Brown, W. A., Frohlich, C., Ellsworth, W., and Luetgert, J. H., 2013, Investigating the Cause of the 17 May 2012 M4.8 Earthquake near Timpson, East Texas: Seismol. Res. Lett., v. 84, no. 2, p. 374.

Chavez, D. E., and Priestley, K. F., 1985, ML Observations in the Great Basin and Mo versus ML Relationships for the 1980 Mammoth Lakes, California, Earthquake Sequence: Bull. Seismol. Soc. Am., v. 75, no. 6, p. 1583-1598.

Cheng, C.-C., and Mitchell, B. J., 1981, Crustal Q Structure in the United States from Multi-mode Surface Waves: Bull. Seismol. Soc. Am., v. 71, no. 1, p. 161-181.

Ebel, J. E., 1982, ML Measurements for Northeastern United States Earthquakes: Bull. Seismol. Soc. Am., v. 72, no. 4, p. 1367-1378.

Erickson, D., McNamara, D. E., and Benz, H. M., 2004, Frequency-Dependent Lg Q within the Continental United States: Bulletin of the Seismological Society of America, v. 94, no. 5, p. 1630-1643.

Fletcher, J. B., and Sykes, L. R., 1977, Earthquakes related to hydraulic mining and natural seismic activity in western New York state: J. Geophys. Res., v. 82, p. 3767-3780.

Frohlich, C., 2012, Two-year survey comparing earthquake activity and injection-well locations in the Barnett Shale, Texas: PNAS.

Frohlich, C., Hayward, C., Stump, B., and Potter, E., 2011, The Dallas-Fort Worth Earthquake Sequence: October 2008 through May 2009: Bull. Seismol. Soc. Amer., v. 101, no. 1, p. 327-340.

Havskov, J., and Ottemoller, L., 1999, SeisAn Earthquake Analysis Software: Seismol. Res. Lett., v. 70, p. 532-534.

Holland, A. A., 2013, Earthquakes Triggered by Hydraulic Fracturing in South-Central Oklahoma: Bull. Seismol. Soc. Am., v. 103, no. 3, p. 1784-1792.

Holland, A. A., Toth, C. R., and Youngblood, A., 2013, Preliminary Analysis of the April 2013 Wellston, Oklahoma, Earthquake Sequence: Oklahoma Geological Survey Open File Report, v. OF1-2013 in prep.

Horton, S., 2012, Disposal of Hydrofacking Waste Fluid by Injection into Subsurface Aquifers Triggers Earthquake Swarm in Central Arkansas with Potential for Damaging Earthquake: Seismol. Res. Lett., v. 83, no. 2, p. 250-260.

Hutton, L. K., and Boore, D. M., 1987, The ML Scale in Southern California: Bull. Seismol. Soc. Am., v. 77, no. 6, p. 2074-2094.

Keranen, K. M., Savage, H. M., Abers, G. A., and Cochran, E. S., 2013, Potentially induced earthquakes in Oklahoma, USA: Links between wastewater injection and the 2011 Mw 5.7 earthquake sequence: Geology.

Kim, W.-Y., 1998, The ML Scale in Eastern North America: Bull. Seismol. Soc. Am., v. 88, no. 4, p. 935-951.

Lienert, B. R. E., and Havskov, J., 1995, A computer program for locating earthquakes both locally and globally: Seismol. Res. Lett., v. 66, p. 26-36.

Miao, Q., and Langston, C. A., 2007, Empirical Distance Attenuation and the Local-Magnitude Scale for the Central United States: Bull. Seismol. Soc. Amer., v. 97, no. 6, p. 2137-2151.

Miller, S. A., Collettini, C., Chiaraluce, L., Cocco, M., Barchl, M., and Kaus, B. J. P., 2004, Aftershocks driven by a high-pressure CO2 source at depth: Nature, v. 247, p. 724-727.

Mitchell, B. J., 1975, Regional Rayleigh Wave Attenuation in North America: Journal of Geophysical Research, v. 80, no. 35, p. 4904-4916.

Nicholson, C., and Wesson, R. L., 1990, Earthquake Hazard Associated With Deep Well Injection -- A Report the the U.S. Environmental Protection Agency: U.S. Geological Survey Bulletin, v. 1951, p. 74.

Nur, A., and Booker, J., 1972, Aftershocks caused by pore fluid flow?: Science, v. 175, no. 885-887.

Nuttli, O. W., 1973, Seismic wave attenuation and magnitude relations for eastern North America: J. Geophys. Res, v. 78, p. 876-885.

Ohtake, M., 1974, Seismic activity induced by water injection at Matsushiro, Japan: J. Phys. Earth, v. 22, p. 163-176.

Richter, C. F., 1935, An Instrumental Earthquake Magnitude Scale: Bull. Seismol. Soc. Am., v. 25, no. 1, p. 32.

Rogers, A. M., Harmsen, S. C., Herrmann, R. B., and Meremonte, M. E., 1987, A Study of Ground Motion Attenuation in the Southern Great Basin, Nevada-California, Using Several Techniques for Estimates of Qs, log Ao, and Coda Q: J. Geophys. Res, v. 92, no. B5, p. 3527-3540.

Rozhko, A. Y., 2010, Role of seepage forces on seismicity triggering: J. Geophys. Res., v. 115.

Rubenstein, J. L., Ellsworth, W. L., and McGarr, A., 2013, The 2001-Present Triggered Seismicity Sequence in the Raton Basin of Southern Colorado/Northern New Mexico: Seismol. Res. Lett., v. 84, no. 2, p. 374.

Savage, M. K., and Anderson, J. G., 1995, A Local-Magnitude Scale for the Western Great Basin-Eastern SierraNevada from Synthetic Wood-Anderson Seismograms: Bull. Seismol. Soc. Am., v. 85, no. 4, p. 1236-1243.

Shapiro, S. A., Audigane, P., and Royer, J. J., 1999, Large-scale in situ permeability tensor of rocks from induced microseismicity: Geophys. J. Int., v. 137, p. 207-213.

Singh, S., and Herman, R. B., 1983, Regionalization of Crustal Coda Q in the Continental United States: Journal of Geophysical Research, v. 88, no. B1, p. 527-538.

Suckale, J., 2009, Induced Seismicity in Hydrocarbon Fields: Advances in Geophysics, v. 51, p. 55-106

Talwani, P., and Acree, S., 1985, Pore Pressure Diffusion and the Mechanism of Reservior-Induced Seismicity: Pageoph, v. 122, p. 947-965.

Uhrhammer, R. A., and Collins, E. R., 1190, Synthesis of Wood-Anderson Seismograms from Broadband Digital Records: Bull. Seismol. Soc. Am., v. 80, no. 3, p. 702-716.

Waldhauser, F., and Ellsworth, W. L., 2000, A double-difference earthquake location algorithm: Method and application to the northern Hayward fault: Bull. Seismol. Soc. Amer., v. 90, p. 1353-1368.

Zoback, M. D., Townend, J., and Grollimund, B., 2002, Steady-state failure equilibrium and deformation of intraplate lithosphere: Internation Geology Review, v. 44.

Appendix A – Local Magnitude Scale used by the OGS

Richter (1935) defined a local-magnitude scale based on recordings from Wood-Anderson torsion seismometer, by defining the maximum amplitude of 1mm measured at a distance of 100 km to be a magnitude 3.0.

$$M_L = logA - logA_0 + 3.0 + S \quad \text{(A.1)}$$

Where A is the measured zero to peak amplitude, $-\log A_0$ represents the attenuation correction factor and S represents a station correction factor. The original M_L relationship derived by Richter (1935) is appropriate for attenuation in Southern California and has been recomputed for Southern California (Hutton and Boore, 1987). The M_L magnitude relationship has been applied to many different regions after the attenuation relationship appropriate for the local region has been modeled. The attenuation correction factor includes the effects of geometrical spreading, anelastic attenuation, and scattering. Examples from the Eastern and Central US include (Ebel, 1982; Kim, 1998; Miao and Langston, 2007). These studies when compared with those in California and the western US (Bakun and Joyner, 1984; Chavez and Priestley, 1985; Rogers et al., 1987; Savage and Anderson, 1995) clearly demonstrate the difference in attenuation between the western US and the stable continental region of the central and eastern US. The greater attenuation of the western US than the central and eastern US is also clearly demonstrated in many studies (Benz et al., 1997; Cheng and Mitchell, 1981; Erickson et al., 2004; Mitchell, 1975; Singh and Herman, 1983).

The recent Earthscope USArray Transportable Array deployment provided an incredible opportunity to both calibrate regional attenuation models for local magnitude, and the relatively dense grid of high-quality broad-band seismic stations also allows us to examine the station corrections and identify regions where attenuation may be different from the regional attenuation model obtained in this study. In this study we have calculated a local magnitude relationship for Oklahoma and the immediately surrounding area. We also examine the spatial distribution of station correction and compare them to the regional geology.

Method

Richter (1935) derived the local-magnitude scale M_L based on seismograms recorded on a standard Wood-Anderson torsion seismometer with free period T_0=0.8 sec, magnification of 2800, and damping of 0.8. Uhrhammer and Collins (1190) determined that the actual magnification of the Wood-Anderson torsion seismometer was 2080 at To=0.8 with a damping of 0.7. This response was used to simulate Wood-Anderson seismograms from regional broad-band stations using the analysis package SEISAN (Havskov and Ottemoller, 1999; Lienert and Havskov, 1995). Hutton and Boore (1987) specified the amplitude measured to be the largest zero to peak amplitude of the S-wave on the horizontal components. This differs from the approach of Richter (1935), which only specified that the largest zero to peak amplitude be used in the determination of M_L. To improve the picking accuracy of amplitudes from synthetic Wood-Anderson seismograms of horizontal components we picked the largest peak to peak amplitude of the S-wave phase and divided the amplitude by 2 to approximate the zero to peak amplitude. We chose to follow the specification of Hutton and Boore (1987) because we wanted an

amplitude based magnitude calculation that would be applicable for locally recorded microearthquakes as well as regionally recorded and felt earthquakes. Consistently using S-waves instead of mixing in Lg phase amplitude measurements allows the separation and comparison with mbLg magnitudes (Nuttli, 1973), which can only be measured at distances greater than 0.5°. It is recognized that S-wave radiation patterns could potentially affect the magnitude for any single event.

In order to determine the local attenuation model for M_L, we follow the method of Miao and Langston (2007), which simultaneously solves for the local attenuation relationship, earthquake magnitudes, and each station components station correction factor. In mathematical notation

$$M_{L_i} = \log A_{ij} + n \log\left(\frac{r_{ij}}{100}\right) + K(r_{ij} - 100) + 3.0 + S_j \qquad \text{(A.2)}$$

where *n* and *K* are parameters describing the local attenuation relationship, and A_{ij} is the amplitude measurement for the *i*th earthquake observed on the *j*th horizontal station component, r_{ij} is the hypocentral distance of *j*th station component to the *i*th earthquake, and *Sj* is the correction for the *j*th station component. In this method the sum of the station residuals is set to zero. The solution was solved using the generalized inverse (Menke, 1989).

Results

In this study we use amplitude measurements from 57 broad-band seismic stations with hypocentral distances less than 450 km, from 341 earthquakes, which provided 8,384 amplitude measurements. The following local magnitude relationship was obtained for the data in this study

$$M_L = \log A + 1.0033 \pm 0.1523 \log\left(\frac{r}{100}\right) - 0.00104 \pm 0.000518(r - 100) + 3.0 \qquad \text{(A.3)}$$

The resulting mean standard deviation for M_L determinations was 0.233 and the mean station correction standard deviation was 0.281. There is a clear dependence on the number of station components measured for a given earthquake and the associated uncertainty in the magnitude with more components yielding a smaller σ, standard deviation.